Published in final edited form as:

Inorg Chem. 2019 March 18; 58(6): 3606–3615. doi:10.1021/acs.inorgchem.8b02160.

Preparation, Characterization, and Electrochemical Activation of a Model [Cp*Rh] Hydride

Emily A. Boyd, **Davide Lionetti**, **Wade C. Henke**, **Victor W. Day**, **James D. Blakemore**

Department of Chemistry, University of Kansas, 1251 Wescoe Hall Drive, Lawrence, KS 66045, USA.

Abstract

Monomeric half-sandwich rhodium hydride complexes are often proposed as intermediates in catalytic cycles, but relatively few such compounds have been isolated and studied, limiting understanding of their properties. Here, we report preparation and isolation of a monomeric rhodium(III) hydride complex bearing the pentamethylcyclopentadienyl (Cp*) and bis(diphenylphosphino)benzene (dppb) ligands. The hydride complex is formed rapidly upon addition of weak acid to a reduced precursor complex, Cp*Rh(dppb). Single-crystal X-ray diffraction data for the [Cp*Rh] hydride, which were previously unavailable for this class of compounds, provide evidence of the direct Rh–H interaction. Complementary infrared spectra show the Rh–H stretching frequency at 1986 cm^{-1}. In contrast to results with other [Cp*Rh] complexes bearing diimine ligands, treatment of the isolated hydride with strong acid does not result in H_2 evolution. Electrochemical studies reveal that the hydride complex can be reduced only at very negative potentials (ca. −2.5 V vs. ferrocenium/ferrocene), resulting in Rh–H bond cleavage and H_2 generation. These results are discussed in the context of catalytic H_2 generation, and development of design rules for improved catalysts bearing the [Cp*] ligand.

Graphical Abstract

blakemore@ku.edu.

ASSOCIATED CONTENT

The following files are available free of charge.

Spectroscopic characterization, electrochemical data, and crystallographic data (PDF)

Cartesian coordinates from crystallography data (XYZ)

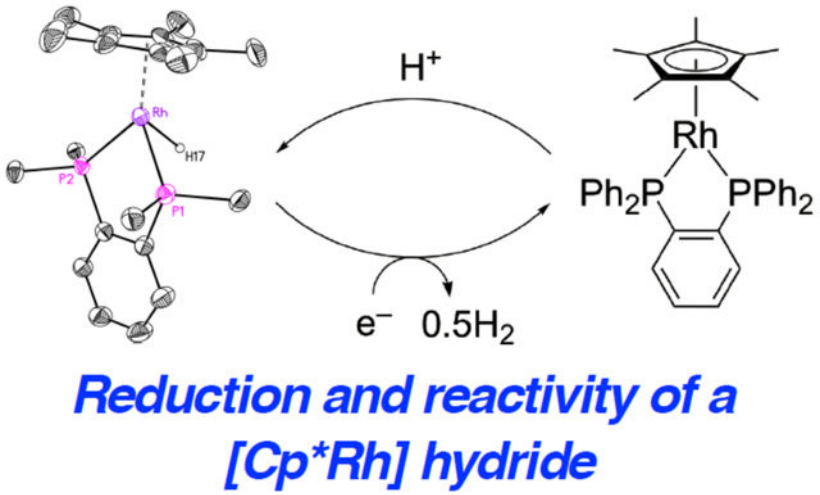

Reduction and reactivity of a [Cp*Rh] hydride

Introduction

Metal hydride complexes are important species in organometallic chemistry.[1] They are key reaction intermediates in many transformations, including hydrogenation of organic molecules, olefin polymerization, and the water-gas shift reaction.[2] They also attract attention in the area of sustainable catalysis, as they are often involved in metal-mediated production of H_2 from water and reduction of CO_2 to more useful chemicals.[3] In these catalytic cycles, however, metal hydrides are often not isolated or even detected directly—rather, their proposed involvement as intermediates is inferred from the observed reactivity.

One such catalytic transformation that has recently attracted significant attention is the chemical or electrochemical generation of H_2 from proton sources that is mediated by [Cp*Rh] complexes (Cp* = pentamethylcyclopentadienyl) supported by bidentate chelating ligands such as 2,2′-bipyridyl and its substituted derivatives. Originally described by Grätzel and Kölle in 1987, this catalyst system is notable for both its ease of preparation from common ligands and readily accessible metal precursors and the stability of the isolated rhodium(III) precatalysts.[4] In cases where catalysis is driven electrochemically, two-electron reduction of the rhodium(III) species in the presence of suitably strong acids (e.g., anilinium triflate, pK_a = 10.6 in CH_3CN[5]) results in quantitative formation of H_2 and regeneration of the rhodium(III) complex.[6] Because of its high efficiency and stability, this catalyst has been deployed in a variety of applications, including attachment to electrode surfaces.[7,8,9]

The mechanism of H_2 generation with this catalyst system was originally proposed to involve two-electron reduction of the precatalyst to generate a rhodium(I) complex that is subsequently protonated to form a [Cp*Rh] hydride species. This hydride complex would then undergo protonolysis, thereby generating H_2.[10] The same hydride intermediate has also been proposed to be involved in generation of NADH from NAD^+ in related work on electrochemically-driven enzymes.[11,12] Signals consistent with the presence of a hydride under stringent reaction conditions (large excess of sodium formate, $Na^+[HCOO]^-$, as hydride source) have been observed by proton nuclear magnetic resonance (^{1}H NMR) in the case of a catalyst supported by 6,6′-dimethyl-2,2′-bipyridyl.[13] The analogous [Cp*Ir]

hydride is well known, and has even been crystallographically characterized, lending credence to the possibility of the involvement of an analogous species in the chemistry of [Cp*Rh] complexes.[14] Nonetheless, despite the proposed involvement of this hydride complex in a number of catalytic mechanisms, neither isolation nor complete *in situ* characterization of this compound has been reported; thus, the involvement of alternate formulations of this protonated species in catalysis cannot be ruled out.

Interest in the [Cp*Rh] systems has recently been refreshed by reports of the generation of η^4-pentamethylcyclopentadiene (Cp*H) complexes under several conditions relevant to H_2 evolution catalysis. Miller and coworkers reported that addition of strong acid (HCl, pK_a < 10.30 in CH_3CN[15]) to Cp*Rh(bpy) results in generation of bound [Cp*H];[16] we have found that the weak acid triethylammonium (pK_a = 18.8 in CH_3CN[5]) can be exploited to cleanly generate complexes bearing [Cp*H] that can subsequently be isolated and stored in pure form on preparative scale (Scheme 1).[17,18] Because of the exclusively *endo* disposition (inward, toward the metal center) of the special ring proton of the [Cp*H] ligand, involvement of Rh in the protonation of the [Cp*] ligand (e.g. as the initial site of protonation) is likely, especially in light of Miller's observation of hydride formation at low temperature followed by [Cp*H] formation upon warming.[16] Hydrogen is quantitatively evolved from this formally rhodium(I) complex bearing [Cp*H] by addition of strong acid, leading to rearomatization of the [Cp*] motif, and suggesting that the protonated ligand complex is not an off-cycle intermediate but rather a species that could be active for catalysis. This notion is supported by a recent computational study, which highlighted the possible protonation pathways in this chemistry and indicated the [Cp*H] species as a lower energy form of the protonated compound vs. the [Rh–H] complex.[19]

As complexes bearing cyclopentadienyl-type ligands are useful in a variety of catalytic applications,[20] the observation of this reversible [Cp*]-centered protonation is of interest for the development of new reactivity manifolds.[21,22] For example, Peters and co-workers have observed ligand-centered protonation of decamethylcobaltocene under conditions relevant to N_2 reduction.[23] The protonated [Cp*] complexes formed in these systems are tautomers of more conventional metal hydrides. Thus, study of isolable [Cp*Rh] hydrides could provide further insights into the chemistry of complexes in this broad family.

Upon investigating this line of research, we were encouraged by literature reports showing that [Cp*Rh] hydride complexes can be stabilized by use of phosphine ligands. Early work from Klingert and Werner showed that treatment of $Cp^*Rh(PMe_3)_2$ with NH_4PF_6 affords $[Cp^*Rh(PMe_3)_2H]^+$.[24] Faller and co-workers later found that an analogous monohydride is sufficiently stable for purification by column chromatography.[25] This finding is complemented by reports of crystallographic characterization of rhodium hydride compounds stabilized by phosphine ligands but not ligated by [Cp*],[26] as well as a more recent report of a crystallographically characterized [Cp^*Fe^{II}] complex stabilized by phosphine ligands.[27] In another key study of interest here, Faraone and co-workers demonstrated preparation of a diphosphine-ligated [CpRh] hydride, although no structural data were collected and the hydride ligand could not be detected by ^1H NMR.[28] Other work from Klingert and Werner includes studies of Rh complexes with bridging PMe_3 ligands.[29,30] Jones has studied the properties of dihydride monophosphine [Cp*Rh] complexes.[31,32]

Lluch, Lledós, and Heinekey investigated a related [Cp*Ir] dihydride with a chelating phosphine ligand, and showed that one [H] ligand was sufficiently hydridic to evolve H_2 by reaction with trace water.[33] However, we are unaware of prior studies of the electrochemical properties of [Cp*Rh] hydride complexes. Such work would complement studies examining reduction of analogous diphosphine [Cp*Rh] complexes without hydride ligands,[10] work with analogous half-sandwich cobalt complexes,[34] and quite recent work from Collomb and co-workers that examined electrochemical H_2 generation pathways in rhodium poly(bipyridyl) complexes.[35]

Here, we describe the isolation and study of a [Cp*Rh] monohydride supported by the bidentate chelate ligand bis(diphenyl)phosphino benzene (dppb). The new complex Cp*Rh(dppb) (**2**) reacts with one or more equivalents of acid to cleanly afford the hydride complex $[Cp^*Rh(dppb)H]^+OTf^-$ (**3**). Electrochemical studies show that this compound is reduced at −2.32 V versus the ferrocenium/ferrocene couple (denoted hereafter $Fc^{+/0}$), giving rise to H_2. Treatment with excess strong acid, in the form of protonated dimethylformamide ($[DMFH]^+$, pK_a = 6.1 in CH_3CN[5]), does not result in hydrogen evolution, even though evolution of hydrogen would be exothermic by 17 kcal/mol based on the electrochemical work. These results are discussed in the context of developing design rules for new catalysts built on the [Cp*Rh] platform.

Results and Discussion

Synthesis of complexes

In order to prepare and study the properties of a monomeric [Cp*Rh] hydride, we selected the bidentate bis(diphenylphosphino)benzene ligand (dppb). This ligand is attractive because it typically binds to a single metal center, forming a relatively stable five-membered chelate ring. [Cp*Rh] complexes bearing bidentate chelating ligands are readily accessible from the versatile, dimeric $[Cp^*RhCl_2]_2$ precursor.[36] Here, addition of 2 equiv. of dppb followed by 2 equiv. of $AgPF_6$ to 1 equiv. of $[Cp^*RhCl_2]_2$ results in formation of the rhodium(III) complex **1** in high yield, along with precipitation of AgCl (Scheme 2).[37]

Vapor diffusion of ether into a concentrated THF solution of **1** yielded orange crystals suitable for single-crystal X-ray diffraction (XRD) studies. The geometry at the formally rhodium(III) center in **1** is pseudo-octahedral, with a first coordination sphere around the metal center containing [Cp*], the expected κ^2-dppb, and a single bound chloride anion (Figure 1). The dppb is forced downward—in the structure of **1**, the angle between the plane containing the [Cp*] ligand and the plane containing Rh, P1, and P2 is 66°; in the analogous $[Cp^*Rh(bpy)Cl]^+$ complex,[38] the angle between the [Cp*] plane and the plane containing Rh and the bound nitrogen atoms is 59°. This suggests that the steric bulk of the dppb framework has a substantial effect on the geometry of the interaction between the bidentate ligand and the [Cp*Rh] motif. We therefore turned to electrochemical methods to establish whether this influence extends to the electronic properties of this species.

The first cathodic sweep of a cyclic voltammogram (CV) of **1** beginning near −0.3 V displays an initial reduction event centered at −0.85 V vs. $Fc^{+/0}$ (Figure 2, upper panel). The peak-to-peak separation of the cathodic and anodic waves is significant (ca. 300 mV),

suggesting a chemical reaction occurs upon reduction. Furthermore, synthetic work (vide infra) and comparison of peak areas in a solution containing a 1:2 mixture of **1** and ferrocene suggests that the reduction of **1** involves transfer of two electrons (Figure S17). This agrees well with prior work on [Cp*Rh] diimine complexes, which typically undergo $2e^-$ reduction near −1.0 V vs. $Fc^{+/0}$.[6,10,39] Indeed, the reduction event for **1** displays the typical profile of an ECE mechanism, in which an initial electrochemical reduction is followed by a chemical reaction (here, a structural rearrangement upon loss of bound chloride) that generates a complex with a more positive reduction potential (i.e., $[Cp^*Rh^{II}(dppb)]^+$). Therefore, a second electron is immediately transferred following the first. A similar profile for this $2e^-$ reduction is observed in voltammetry across a range of scan rates (see Figure S18 in SI), suggesting that the coupled chemical reactions are reasonably fast on the timescale of voltammetry. The observed peak currents for both the reduction and oxidation events vary linearly with the square root of scan rate, confirming both the oxidized and reduced forms of **1** are soluble and freely diffusing (Figure S18). Notably, we observed no further reductions with **1** within the limit of our conditions, down to potentials around −2.5 V (Figure S19, lower panel, in SI).

In the second and subsequent cycles of voltammetry, a new reductive feature appears at slightly more positive potential than the dominant reduction wave (See Figures S18 and S19 in the SI). Specifically, a small new reductive wave appears with $E_{p,c} = -0.82$ V. The appearance of this wave upon multiple cycling is consistent with initial reduction of **1** (virtually all chloride-bound when dissolved in the electrolyte solution) by two electrons to form **2** (Scheme 2). Subsequent re-oxidation and ligand coordination can result in two possible products, chloride-bound **1** or the analogous solvento complex, $[Cp^*Rh(dppb)(NCMe)]^{2+}$. The small, additional reductive wave thus corresponds to two-electron reduction of $[Cp^*Rh(dppb)(NCMe)]^{2+}$ to form **2**. The shift in reduction potential for the solvento species is consistent with analogous observations in bpy-supported Co, Rh, and Ir systems.[40]

This electrochemical response is reminiscent of that of [Cp*Rh] complexes bearing bpy or related 4,4′-disubstituted 2,2′-bipyridyl ligands.[6,41] In the case of the parent bpy system, a single $2e^-$, ECE-type reduction event gives rise to a five-coordinate $18e^-$ species.[4] The five-coordinate complex Cp*Rh(bpy) has been chemically prepared and structurally characterized, confirming its identity as the product of reduction of the rhodium(III) starting material. Notably, this formally rhodium(I) complex displays significant delocalization of electron density into the π-system of the bpy ligand, as judged by single-crystal XRD and UV-visible spectroscopy.[42]

In accord with the two-electron reduction of **1** observed by cyclic voltammetry, treatment of a THF suspension of **1** with sodium amalgam ($E° \approx -2.4$ V[43], 10 equiv.) results in generation of **2**. Over the course of the reaction, the solution darkens considerably in color. Following work-up and extraction with hexanes, diamagnetic **2** can be isolated in pure form. Characterization of **2** by ^{1}H NMR (Figure S6) indicates retention of both the [Cp*] and dppb ligands, as the 15 equivalent protons of the freely rotating [Cp*] ring show coupling to the two equivalent bound phosphorus atoms ($^3J_{H,P} = 1.8$ Hz), similar to data collected for **1** ($^3J_{H,P} = 3.4$ Hz). $^{31}P\{^1H\}$ NMR spectra support assignment of reduction of the rhodium metal center; $^1J_{P,Rh}$ increases from 131 Hz in **1** to 220 Hz in **2**, in accord with formation of a

more electron-rich rhodium center (Figure 3) which can engage in backdonation to the π-acidic phosphine ligands. The phosphine resonances also shift downfield (ca. 9 ppm) upon reduction. Crystals of this complex suitable for XRD studies could not be obtained due to the high solubility of this species in most organic solvents. However, as the ^{1}H NMR does not indicate the presence of additional ligands bound to the Rh center, we conclude that this complex, similar to Cp*Rh(bpy), is a five-coordinate, 18e^{-} complex.

Cyclic voltammetry data obtained with isolated **2** confirm that this compound is the product of electrochemical reduction of **1** (Figure 2, lower panel). Starting the initial anodic sweep from reducing potentials, we observe a sole oxidation wave ($E_{p,a}$ = −0.73 V) coupled to a sole reduction wave ($E_{p,c}$ = −0.82 V). This two-electron event is centered at −0.78 V vs. Fc$^{+/0}$, slightly more positive than the rhodium(III/I) couple measured for the chloride-containing starting material **1** (Figure 2, upper panel). This is consistent with generation of the more oxidizing [Cp*Rh(dppb)(NCMe)]$^{2+}$ upon 2e^{-} oxidation of **2**. Similarly, the reduction wave measured for this solvento complex generated from **2** *in situ* (Figure S18) is shifted positive from the reduction wave measured for chloride-bound **1**. Scan rate-dependent studies confirm that **2**, and its oxidation product [Cp*Rh(dppb)(NCMe)]$^{2+}$, are freely diffusing, soluble species (Figure S20).

With **2** in hand, we explored the possibility of generating a hydride species by treatment of **2** with acid. For the analogous Cp*Rh(bpy) system, treatment with triethylammonium bromide (pK_a = 18.8 in CH_3CN[5]) results in generation of the isolable (Cp*H)Rh(bpy)Br complex.[18] However, as **2** has a more positive reduction potential than Cp*Rh(bpy), we targeted the stronger acid anilinium triflate (pK_a = 10.6 in MeCN[5]) for generation of a singly-protonated complex.[44] Indeed, treatment of **2** in MeCN with 1.0 equiv. of anilinium triflate results in a visible lightening of the solution without formation of a visible precipitate. Following work up, ^{1}H NMR reveals a distinctive new signal at −11.8 ppm consistent with formation of a metal hydride species (**3**; see Figure S10). This signal appears as a quartet (rather than the expected doublet of triplets or triplet of doublets) due to an apparent coincidental similarity in the H,Rh and H,P coupling constants (i.e., $^{1}J_{H,Rh} \approx {}^{2}J_{H,P} \approx 29$ Hz). Importantly, whereas proton transfer to [Cp*] in [(Cp*H)Rh(bpy)]$^{+}$ results in three inequivalent methyl resonances in its ^{1}H NMR spectrum (a doublet and two singlets are observed),[16,17] a single resonance for the [Cp*] protons is present in data for **3** (Figure S10), excluding generation of any [Cp*H] species or free pentamethylcyclopentadiene. ^{31}P{^{1}H} spectra of **3** (see Figures 3 and S13) confirm formation of a new complex–a lone doublet at 67.9 ppm ($^{1}J_{P,Rh}$ = 138 Hz) is observed, consistent with a rhodium(III) species. (See SI for additional NMR spectra related to characterization of **3**.) In accord with all these data, the infrared spectrum of **3** shows a distinctive [Rh–H] stretch at 1986 cm^{-1} (see Figure S28 in SI).

Vapor diffusion of diethyl ether into a concentrated solution of **3** in THF yielded small light-yellow crystals suitable for XRD studies. The geometry at the formally rhodium(III) metal center is again pseudo-octahedral, with dppb retained in the κ^{2} mode and [Cp*] bound in the typical η^{5} mode. (Figure 4). [Cp*] is planar, indicating that it retains its aromatic nature and no [Cp*H] material has formed. Gratifyingly, the hydride ligand (H17) was located in the Fourier difference map, and its position was freely refined. H17 is bound to the rhodium center, confirming the generation of a metal hydride moiety.[45]

Chemical Properties of the [Cp*Rh] Hydride

As discussed above, treatment of the isolated protonated species $[(Cp^*H)Rh(bpy)]^+$ with strong acid ($[DMFH]^+[OTf]^-$) results in rapid generation of H_2 concurrent with a color change indicative of consumption of the Rh(I) species and generation of $[Cp^*Rh(bpy)]^{2+}$.[18] In the case of **3**, however, addition of $[DMFH]^+[OTf]^-$ does not lead to any detectable reactivity over 48 h as determined by ^{1}H NMR spectroscopy (Figure 5). Heating such a sample at 50°C overnight also does not lead to reactivity. The resistance of **3** to protonolysis (H_2 evolution by direct protonation) even by strong H^+ sources highlights stability of this protonated species as compared to that of $[(Cp^*H)Rh(bpy)]^+$. Storage of the first H^+ equivalent on the [Cp*] ring, evidently enabled by bpy but disfavored by dppb, appears to promote further reaction with H^+ to generate H_2.

The stability of **3** towards H^+ sources is reminiscent of that of analogous [Rh–CH_3] complexes supported by [Cp*] and bpy that we have recently studied.[39] These rhodium–methyl species can be dissolved in neat methanol (MeOH) without detectable protonolysis of the CH_3 ligand. However, these complexes are susceptible to reaction with stronger H^+ sources (e.g., $[DMFH]^+[OTf]^-$) leading to generation of CH_4.[40] It has been noted that Rh–C bonds can be quite strong,[46] but prior observations suggest that M–H bonds tend to be stronger than their M–C analogues.[47]

Calculation of the difference between the estimated thermodynamic potential required for H_2 evolution with $[DMFH]^+[OTf]^-$ ($E^{o\prime}(H^+/H_2) = -0.389$ V)[43] and the reducing power of the Cp*Rh(dppb) complex ($E_{1/2}(Rh^{III}/Rh^{I}) = -0.78$ V) reveals that H_2 evolution would be substantially exergonic, with a driving force of ca. 17 kcal mol^{-1}.[44,48,49] Therefore, the inability of the dppb-supported system to generate H_2 even in the presence of excess $[DMFH]^+[OTf]^-$ could provide insight into the mechanism of H_2 evolution by other [Cp*Rh] species. Complexes containing diimine ligands are competent electrocatalysts for H_2 evolution; we have recently reported that introduction of substituents on the bpy framework affects the catalytic performance but leads to observation of [Cp*H] species as the primary product of protonation of the respective Rh(I) complexes, analogously to the parent bpy system.[6]

In terms of the potential required for charging of the catalyst with the required reducing equivalents, the Cp*Rh(diimine) complexes in our previous studies[6] are more potent reducing agents ($E_{1/2}(Rh^{III}/Rh^{I}) \leq -0.97$ V) than **2** ($E_{1/2}(Rh^{III}/Rh^{I}) = -0.78$ V). Although this factor may contribute to the lack of catalysis with **2**, it should be noted that the overpotential for the H_2 evolution from **2** with $[DMFH]^+$ as acid is essentially equivalent ($\eta \approx 0.38$ V) to that for H_2 evolution from Cp*Rh(bpy) with anlinium as proton source. This observation suggests that the differences in the observed catalytic performance of these two systems could arise from changes in their chemical reactivity (e.g., protonation at the metal vs. on the Cp* ligand), rather than simply from their differing reducing power.

However, we have recently observed partial formation of Rh–H species with diimine-based complexes by ^{1}H NMR spectroscopy. Specifically, we observe minor hydride signals *in situ* when we treat Rh(I) starting materials (e.g., Cp*Rh(^{R}bpy), ^{R}bpy = 4,4'-R_2-bpy, R = ^{t}Bu, H, CF_3) with $[C_6H_5NH_3]^+$ (anilinium, pK_a = 10.6 in MeCN[5]) as proton source; upfield

resonances around −9 ppm (see Figure S15 in SI) are indicative of Rh–H moieties; these signals are similar to those in prior reports of a hydride detected at low temperature[16] and another under aqueous conditions.[13] Observation of hydride species in the presence of anilinium/aniline suggests that an external proton transfer mediator may lower a kinetic barrier for interconversion of the two tautomers (i.e., [(Cp*H)Rh^{I}] and [Cp*Rh^{III}–H]). Our prior computational study found a low-lying transition state to transfer [H] from Rh to the Cp* ring (the [Cp*H] complex being the lower energy structure in comparison to the analogous [Rh^{III}–H]), although involvement of H-bond donors and acceptors in metal-to-ring or ring-to-metal [H] transfer remains to be further explored.[19] In the case of experiments involving anilinium/aniline, the presence of additional protons on the conjugate base (cf., Et_3N in prior modeling studies[19]) could facilitate simultaneous proton transfer to and from the base, complicating study of equilibria with this stronger acid. Further discernment of the thermochemical parameters and kinetic barriers involved in evolution of H_2 from [Cp*Rh] complexes bearing diimine ligands thus remains of interest.

Comparisons between the speciation profile and subsequent reactivity of the Cp*Rh(^{R}bpy) systems and of the present dppb-supported complex may shed light upon the possible mechanisms of H_2 evolution in this family of catalysts. Upon protonation of Rh(I) complexes supported by ^{tBu}bpy and ^{H}bpy, both competent H_2 evolution catalysts at their respective Rh(III/I) couples, hydride signals are observed in the presence of aniline/anilinium (Figure S15). On the other hand, protonation of the Rh(I) complex supported by ^{CF3}bpy does not give rise to any detectable hydride species; this system is also a poor catalyst at the potential of its Rh(III/I) couple, and only displays appreciable catalysis upon further reduction.[6] In the present system supported by the dppb ligand, hydride complex **3** is the only product of protonation of the corresponding Rh(I) species **2** (i.e., no (Cp*H)-containing species are observed) and the system is not a catalyst for H_2 evolution. Notably, the two sets of complexes that display a single product upon protonation also display attenuated (or completely absent) catalysis at their respective Rh(III/I) couples. These observations are in good agreement with the results of computational studies on the mechanism of proton transfer in these systems, which implicated acid-dependent mechanisms of H_2 evolution via intermediates in which the first H^+ equivalent delivered "bridges" between the metal center and the [Cp*] ring.[19]

Within this paradigm, the ability of the protonated species to access "bridging" states between the [(Cp*H)Rh] and [Rh–H] extremes appears to be key to promoting catalytic behavior. Excessive stabilization of either motif ([(Cp*H)Rh] by ^{CF3}bpy, [Rh–H] by dppb) introduces a barrier to further reactivity that cannot be overcome under the conditions studied. Thus, by tuning the relative (differential) basicity of the two sites that can be involved in proton transfer (the Rh center and the [Cp*] ring), the supporting bidentate ligands (bpy, dppb) play a key role in directing reactivity along distinct manifolds. The stark contrast between the robust catalysis of select Cp*Rh(diimine) complexes and the inertness of Cp*Rh(dppb) toward H_2 evolution suggests that a design rule for catalysis of small-molecule transformations with [Cp*Rh] complexes could be a requirement for enabling access to both [Cp*H] intermediates and Rh–H complexes rather than strong stabilization of one of these forms over the other.

Electrochemical Properties of the [Cp*Rh] Hydride

Having observed that **3** does not react with even strong acids, we were interested in the electrochemical properties of this apparently stable compound. Initially, we moved to confirm that there is no electrocatalytic generation of H_2 driven by formation of the Rh^{III}–H species (**3**). For example, addition of $[C_6H_5NH_3][OTf]$ to an electrochemical cell containing **1** results in loss of reversibility for the $2e^-$ wave observed by cyclic voltammetry (see SI, Figure S21). This is consistent with generation of the hydride species **3** in a chemical reaction between electrochemically generated **2** and H^+. However, there is no catalytic enhancement above the electrode background in these studies at relevant potentials, even in the presence of excess acid (see SI for details). This result contrasts with our prior work on Cp*Rh(diimine) complexes under similar conditions.[6]

However, interrogation of isolated **3** suggests that further reduction of the hydride complex is possible. In the CV of isolated **3**, a cathodic wave is observed at −2.34 V vs. $Fc^{+/0}$, near the limit of polarization for our conditions (Figure 6). A small corresponding anodic wave is observed at −2.24 V, suggesting that the electrochemical reduction of **3** is followed by a chemical reaction (in an EC-type process). In accord with this theory, increasing the voltammetric scan rate (see SI, Figure S22) results in improved electrochemical reversibility, and suggests an approximate midpoint potential for $1e^-$ reduction of **3** near −2.29 V. The peak current for the reduction event varies linearly with the square root of scan rate, in accord with the soluble and freely diffusing nature of **3**. A new anodic wave, absent during the initial scan, appears at $E_{p,c}$ = −0.73 V after these cathodic scans (Figure 6 and S19). The potential for this new process is virtually identical to that for oxidation of Rh(I) complex **2** to the corresponding solvento Rh(III) species (Figure 2, lower panel); this observation suggests that reduction of **3** leads to partial loss of the hydride ligand and concomitant regeneration of the non-protonated species **2**.

These results are analogous to the observation of a $1e^-$ reduction event ($E_{p,c}$ = −1.45 V) in the CV of $[(Cp^*H)Rh(^{CF3}bpy)]^{2+}$ (^{CF3}bpy = 4,4’-di(trifluromethyl)-2,2’bipyridine).[6] Reduction of this species can lead to generation of H_2 (0.5 equiv per Rh complex) and formation of $Cp^*Rh(^{CF3}bpy)$, consistent with net formal loss of a hydrogen atom (H•). An analogous reduction was observed in [(Cp*H)Rh(bpy)Br] ($E_{p,c}$ = −1.73 V) and leads to a similar H_2 evolution pathway; chemical reactivity and bulk electrolysis experiments confirmed generation of Cp*Rh(bpy) and H_2 upon $1e^-$ reduction of [(Cp*H)Rh(bpy)Br].[18] Thus, we propose that reduction of **3** leads to release of H_2 and regeneration of Rh(I) complex **2**, according to the following equation (eq. 1):

$$2[Cp^*Rh(dppb)H]^+ + 2e^- \rightarrow H_2 + 2Cp^*Rh(dppb) \quad \text{(eq.1)}$$

To test this hypothesis, we targeted both bulk electrolysis and chemical reduction experiments to determine the products of reduction of **3**. Controlled potential electrolysis of **3** was carried out at −2.23 V vs. $Fc^{+/0}$ (Figure S23) for 1.1 h; headspace analysis by gas chromatography (GC) revealed the presence of H_2 with a 58% Faradaic yield. The primary metal-containing product of the electrolysis was identified as **2** via UV-visible spectroscopy (see Figure S25 and further experimental information in SI for details). Similarly, treatment

of **3** with 1 equiv of sodium naphthalenide (Na[C_8H_{10}], $E°$ = −3.10 V)[42] results in a color change from light yellow to dark red in seconds, suggesting generation of **2**. Headspace analysis by GC confirms generation of H_2 upon chemical reduction. Consistent with the electrochemical work, the primary metal-containing product of the reduction was identified as **2** via $^{31}P\{^1H\}$ NMR spectroscopy (Figure S16).

Thus, despite the resistance of Rh–H complex **3** to protonolysis, generation of H_2 from this complex can be achieved via 1e$^-$ reduction (Figure 7). This process is analogous to the catalytic H_2 evolution that can be induced by reduction of [Cp*H] complexes supported by bpy[18] and ^{CF3}bpy,[6] as well as H_2 evolution mechanisms that have been demonstrated for cobaloximes,[50] [Cp*Ir(bpy)H]$^+$,[51] and poly(bipyridyl) rhodium hydrides.[35] However, we note that the modest Faradaic yield of H_2 measured following electrolysis of **3** contrasts with the near unity yield encountered in our work with the bpy and ^{CF3}bpy complexes. We ascribe this diminished efficiency to side reactions that can occur in the case of chemical and electrochemical reduction of **3**.

The reductions of the rhodium complexes bearing [Cp*H] are centered on the bpy ligands, due to the low-lying, delocalized bpy **π*** orbitals. As a result, these processes occur at substantially more positive potentials (−1.73 and −1.45 V, respectively) than the reduction measured for **3** (−2.34 V).[52] Thus, we propose that the reduction of **3** is likely to be metal-centered, leading to generation of a reactive (transient) Rh^{II}–H complex that could undergo Rh–H bond homolysis or protonolysis by an exogenous H^+ source. The notion of a transient Rh^{II} complex is consistent with the appearance of a small anodic wave ($E_{p,a}$ = −2.24 V) coupled to reduction of **3** (see Figure 6). For comparison, the free dppb ligand is reduced at a more negative potential,[53] while other metal complexes of dppb do not manifest ligand-centered reductions at relevant potentials.[54,55] Our proposal is also consistent with electrochemical studies of the related [Cp*Rh(bpy)Me]$^+$ complex which undergoes both quasi-reversible diimine-centered reduction ($E_{1/2}$ = −1.78 V) and metal-centered reduction ($E_{p,c}$ = −2.22 V), as demonstrated by chemical and spectroscopic studies.[40] And, although we have not investigated the mechanism of H_2 generation from this system further, we note that a bimolecular pathway leading to H_2 generation with **3** via bond homolysis of a transient [Rh^{II}–H] species would be reminiscent of Wayland's generation of [Rh^{III}–H]$_2$ species by treatment of bimetallic [Rh^{II}_2] complexes with H_2.[56]

Conclusions

The rhodium half-sandwich complex Cp*Rh(dppb) reacts with acid to form an isolable monohydride, [Cp*Rh(dppb)H]$^+$OTf$^-$. There is no evidence of generation of coordinated pentamethylcyclopentadiene, [Cp*H], or free Cp*H, under these conditions, in accord with formation of a Rh–H bond. This interaction is apparently quite stable, as the hydride complex is not protonated by the strong acid DMFH$^+$ to yield H_2 over 48 h of monitoring by NMR. However, the isolated hydride undergoes reduction at −2.34 V, leading to generation of H_2 and formation of Cp*Rh(dppb). Taken together, these studies suggest that [Cp*Rh^{III}] hydride complexes can be remarkably stable species. Because of the observed formation of [Cp*H] upon protonation of analogous [Cp*Rh] diimine complexes, a possible design rule for improved catalysis involving proton-driven transformations may be use of ligands that

enable ligand-centered protonation. Our ongoing work is examining use of this strategy to promote new reactivity with these robust and useful compounds.

Experimental Section

General Considerations

All manipulations were carried out in dry N_2-filled gloveboxes (Vacuum Atmospheres Co., Hawthorne, CA) or under N_2 atmosphere using standard Schlenk techniques unless otherwise noted. All solvents were of commercial grade and dried over activated alumina using a PPT Glass Contour (Nashua, NH) solvent purification system prior to use, and were stored over molecular sieves. All chemicals were from major commercial suppliers and used as received after extensive drying. $[Cp^*RhCl_2]_2$ was prepared according to the literature procedure.[36] Deuterated NMR solvents were purchased from Cambridge Isotope Laboratories; CD_3CN was dried over CaH_2 and C_6D_6 was dried over sodium/benzophenone. ^1H, ^{13}C, ^{19}F, and ^{31}P NMR spectra were collected on 400 or 500 MHz Bruker spectrometers and referenced to the residual protio-solvent signal[57] in the case of ^1H and ^{13}C. Heteronuclear NMR spectra were referenced to the appropriate external standard following the recommended scale based on ratios of absolute frequencies (Ξ).[58,59] ^{19}F NMR spectra are reported relative to CCl_3F, and ^{31}P NMR spectra are reported relative to H_3PO_4. Chemical shifts (δ) are reported in units of ppm and coupling constants (*J*) are reported in Hz. Electronic absorption spectra were collected with an Ocean Optics Flame spectrometer, in a 1-cm pathlength quartz cuvette. Elemental analyses were performed by Midwest Microlab, Inc. (Indianapolis, IN).

Electrochemistry

Electrochemical experiments were carried out in a nitrogen-filled glovebox. 0.10 M tetra(n-butylammonium) hexafluorophosphate (Sigma-Aldrich; electrochemical grade) in acetonitrile served as the supporting electrolyte. Measurements were made with a Gamry Reference 600 Plus Potentiostat/Galvanostat using a standard three-electrode configuration. The working electrode was the basal plane of highly oriented pyrolytic graphite (HOPG) (GraphiteStore.com, Buffalo Grove, Ill.; surface area: 0.09 cm^2), the counter electrode was a platinum wire (Kurt J. Lesker, Jefferson Hills, PA; 99.99%, 0.5 mm diameter), and a silver wire immersed in electrolyte served as a pseudo-reference electrode (CH Instruments). The reference was separated from the working solution by a Vycor frit (Bioanalytical Systems, Inc.). Ferrocene (Sigma Aldrich; twice-sublimed) was added to the electrolyte solution at the conclusion of each experiment (~1 mM); the midpoint potential of the ferrocenium/ferrocene couple (denoted as $Fc^{+/0}$) served as an external standard for comparison of the recorded potentials. Concentrations of analyte for cyclic voltammetry were typically 1 mM.

Synthetic Procedures

Synthesis of 1.—To a suspension of $[Cp^*RhCl_2]_2$ in CH_2Cl_2 (0.0678 g, 0.109 mmol) were added dppb (0.1004 g, 0.224 mmol, 2.05 equiv) and $AgPF_6$ (0.0552 g, 0.219 mmol, 2 equiv) as CH_2Cl_2 solutions. The color of the reaction mixture rapidly changed from brick-red to orange, and a colorless precipitate formed. After 15 min, the suspension was filtered to remove the AgCl byproduct, and the volume of the filtrate was reduced to ~1 mL.

Addition of Et_2O (~20 mL) caused precipitation of a yellow solid, which was collected by filtration. Pure material was obtained via crystallization by vapor diffusion of Et_2O into a concentrated THF solution of the title compound (0.149 g, 78%). The same strategy was employed to obtain single-crystals suitable for X-ray diffraction studies. ^{1}H NMR (500 MHz, CD_3CN) δ 7.82 (m, 4H, *H8*), 7.77 (m, 2H, *H12*), 7.72 (t, *J* = 7.9 Hz, 2H, *H10*), 7.64 (m, 2H, *H13*), 7.61 (t, *J* = 7.6 Hz, 4H, *H9*), 7.53 (t, *J* = 7.57 Hz, 2H, *H6*), 7.29 (td, *J* = 8.0, 1.8 Hz, 4H, *H5*), 6.91 (ddt, *J* = 9.5, 6.2, 1.4 Hz, 4H, *H4*), 1.56 (t, *J* = 3.4 Hz, 15H, *H1*) ppm. $^{13}C\{^1H\}$ NMR (126 MHz, CD_3CN) δ 134.27 (t, *J* = 5.31 Hz, *C8*), 132.52 (t, *J* = 5.8 Hz, *C4*), 131.67 (m), 131.48 (m), 131.2 (m), 128.07 (t, *J* = 5.7 Hz, *C5*), 127.73 (t, *J* = 6.0 Hz, *C9*), 104.39 (dt, *J* = 5.6, 2.7 Hz, *C2*), 7.91 (m, *C1*) ppm. ^{19}F NMR (376 MHz, CD_3CN) δ −73.77 (d, $^1J_{F,P}$ = 706 Hz) ppm. $^{31}P\{^1H\}$ NMR (162 MHz, CD_3CN) δ 58.32 (d, $^1J_{P,Rh}$ = 129.9 Hz, dppb), −147.65 (sept, $^1J_{P,F}$ = 706 Hz) ppm. (See Figure S1 in SI showing the labeling scheme for the carbon and hydrogen atoms.) Electronic absorption spectrum (THF): 362 (7,500 M^{-1} cm^{-1}). Anal. Calcd. for $C_{40}H_{39}ClF_6P_3Rh$: C, 55.54; H, 4.55. Found: C, 54.69; H, 4.59. The low carbon value is attributed to association of water, which is consistent with the presence of water in the ^{1}H NMR spectrum of **1**.

Synthesis of 2.—A suspension of **1** in THF (0.1022 g, 0.118 mmol) was stirred over freshly prepared sodium-mercury amalgam (1% Na in Hg; 0.0273 g Na^0, 1.18 mmol, 10 equiv) for 24 hours, during which time the yellow suspension became a dark red homogeneous solution. The mixture was filtered and the volatiles removed *in vacuo*. Extraction with Et_2O and removal of the volatiles *in vacuo* provides the title compound as a dark red solid (0.0690 g, 85%). ^{1}H NMR (400 MHz, C_6D_6) δ 7.81 (m, 8H), 7.54 (m, 2H), 7.14 (t, *J* = 7.39 Hz, 8H, overlaps with solvent residual), 7.06 (t, *J* = 6.61 Hz, 4H), 6.82 (m, 2H), 1.79 (t, *J* = 1.8 Hz, 15H, Cp*) ppm. ^{13}C NMR (126 MHz, C_6D_6) δ 149.63 (td, *J* = 46.78, 3.46 Hz), 138.75 (t, *J* = 18.67 Hz), 133.37 (t, *J* = 6.5 Hz), 130.27 (t, *J* = 9.1 Hz), 129.10, 128.75, 127.52 (obscured by solvent peak), 96.06 (m), 10.84 ppm. ^{31}P NMR (162 MHz, C_6D_6) δ 76.63 (d, $^1J_{P,Rh}$ = 219.5 Hz) ppm. $^{31}P\{^1H\}$ NMR (162 MHz, C_6D_6) δ 76.63 (d, $^1J_{P,Rh}$ = 220.0 Hz) ppm. Electronic absorption spectrum (THF): 393 (4,800), 478 (2,500 M^{-1} cm^{-1}).

Synthesis of 3.—A solution of anilinium triflate in thawing MeCN (0.0272 g, 0.112 mmol, 1 equiv) was added dropwise to a solution of **2** in THF (0.0765 g, 0.112 mmol). The solution became light yellow immediately. Volatiles were removed *in vacuo*. Washing with hexanes, Et_2O, and toluene followed by extraction with THF and removal of volatiles yielded the title compound as a light-yellow solid (0.0812 g, 87%). Single-crystals suitable for X-ray diffraction studies were obtained by vapor diffusion of Et_2O into a THF solution of the title compound. ^{1}H NMR (400 MHz, CD_3CN) δ 7.71–7.57 (m, 12H), 7.54–7.48 (m, 4H), 7.38 (td, *J* = 7.9, 1.9 Hz, 4H), 7.15 (ddt, *J* = 11.8, 8.0, 1.4 Hz, 4H), 1.58 (td, *J* = 2.9, 1.1 Hz, 15H), −11.78 (q, *J* = 29.2 Hz, 1H, hydride) ppm. $^{13}C\{^1H\}$ NMR (126 MHz, CD_3CN) δ 132.38 (t, *J* = 6.2 Hz), 131.98 (t, *J* = 6.3 Hz), 131.18 (m), 130.99 (m), 130.77 (m), 130.48 (t, *J* = 9.2 Hz), 128.30 (t, *J* = 6.0 Hz), 128.00 (t, *J* = 5.7 Hz), 101.57 (dt, *J* = 4.6, 2.4 Hz, Rh–*C*5(CH3)5), 8.16 (s, Rh–C5(*C*H3)5) ppm. ^{19}F NMR (376 MHz, CD_3CN) δ −80.21 (s) ppm. $^{31}P\{^1H\}$ NMR (162 MHz, CD_3CN) δ 67.12 (d, $^1J_{P,Rh}$ = 137.8 Hz). Electronic absorption spectrum (THF): 305 (15,900 M^{-1} cm^{-1}). Anal. Calcd. for $C_{41}H_{40}O_3F_3P_2SRh$: C, 59.00; H,

4.84. Found: C, 59.70; H, 4.94. The high carbon value is attributed to association of THF, which is consistent with the presence of THF in the ^{1}H NMR spectrum of **3**.

Supplementary Material

Refer to Web version on PubMed Central for supplementary material.

Acknowledgements

The authors thank Justin Douglas and Sarah Neuenswander for assistance with NMR spectroscopy. This work was supported by the University of Kansas. E.A.B. acknowledges the Center for Undergraduate Research at the University of Kansas for support in the form of an Undergraduate Research Award. Support for NMR instrumentation was provided by NIH Shared Instrumentation Grants S10OD016360 and S10RR024664, and by an NSF MRI Grant CHE-1625923.

References

1. Kaesz HD; Saillant RB Hydride Complexes of the Transition Metals. Chem. Rev 1972, 72, 231–281.
2. Jordan AJ; Lalic G; Sadighi JP Coinage Metal Hydrides: Synthesis, Characterization, and Reactivity. Chem. Rev 2016, 116, 8318–8372. [PubMed: 27454444]
3. Rakowski Dubois M; Dubois DL Development of Molecular Electrocatalysts for CO_2 Reduction and H_2 Production/Oxidation. Acc. Chem. Res 2009, 42, 1974–1982. [PubMed: 19645445]
4. Kölle U; Grätzel M Rhodium(III) Complexes as Homogeneous Catalysts for the Photoreduction of Protons to Hydrogen. Angew. Chem 1987, 99, 572–574.
5. Muckerman JT; Skone JH; Ning M; Wasada-Tsutsui Y Toward the Accurate Calculation of pK_a Values in Water and Acetonitrile. Biochim. Biophys. Acta Bioenerg 2013, 1827, 882–891.
6. Henke WC; Lionetti D; Moore WNG; Hopkins JA; Day VW; Blakemore JD Ligand Substituents Govern the Efficiency and Mechanistic Path of Hydrogen Production with [Cp*Rh] Catalysts. ChemSusChem 2017, 10, 4589–4598. [PubMed: 29024563]
7. Cosnier S; Deronzier A; Vlachopoulos N Carbon/poly[pyrrole-[(C_5Me_5)Rh(III)(bpy)Cl]$^+$] Modified Electrodes; a Molecularly-Based Material for Hydrogen Evolution (bpy = 2,2'-bipyridine) J. Chem. Soc., Chem. Commun 1989, 1259–1261.
8. Caix C; Chardon-Noblat S; Deronzier A; Moutet J-C; Tingry S (Pentamethylcyclopentadienyl) (polypyridyl)rhodium and Iridium Complexes as Electrocatalysts for the Reduction of Protons to Dihydrogen and the Hydrogenation of Organics. J. Organomet. Chem 1997, 540, 105–111.
9. Blakemore JD; Gupta A; Warren JJ; Brunschwig BS; Gray HB Noncovalent Immobilization of Electrocatalysts on Carbon Electrodes for Fuel Production. J. Am. Chem. Soc 2013, 135, 18288–18291. [PubMed: 24245686]
10. Kölle U; Kang BS; Infelta P; Comte P; Grätzel M Electrochemical and Pulse-Radiolytic Reduction of (Pentamethylcyclopentadienyl)(polypyridyl)rhodium Complexes. Chem. Ber 1989, 122, 1869–1880.
11. Ruppert R; Herrmann S; Steckhan E Efficient Indirect Electrochemical in situ Regeneration of NADH: Electrochemically Driven Enzymatic Reduction of Pyruvate Catalyzed by D-LDH. Tet. Lett 1987, 28, 6583–6586.
12. Lo HC; Leiva C; Buriez O; Kerr JB; Olmstead MM; Fish RH Regioselective Reduction of NAD^+ Models, 1-Benzylnicotinamide Triflate and β-Nicotinamide Ribose-5'-methyl Phosphate, with in Situ Generated $[CpRh(Bpy)H]^+$: Structure-Activity Relationships, Kinetics, and Mechanistic Aspects in the Formation of the 1,4-NADH Derivatives. Inorg. Chem 2001, 40, 6705–6716. [PubMed: 11735482]
13. Steckhan E; Herrmann S; Ruppert R; Dietz E; Frede M; Spika E Analytical Study of a Series of Substituted (2,2'-bipyridyl)(pentamethylcyclopentadienyl)rhodium and -iridium Complexes with Regard to their Effectiveness as Redox Catalysts for the Indirect Electrochemical and Chemical Reduction of $NAD(P)^+$. Organometallics 1991, 10, 1568–1577.

14. Abura T; Ogo S; Watanabe Y; Fukuzumi S Isolation and Crystal Structure of a Water-Soluble Iridium Hydride: A Robust and Highly Active Catalyst for Acid-Catalyzed Transfer Hydrogenations of Carbonyl Compounds in Acidic Media. J. Am. Chem. Soc 2003, 125, 4149–4154. [PubMed: 12670237]
15. Kütt S; Rodima T; Saame J; Raamat E; Mäemets V; Kaljurand I; Koppel IA; Garlyauskayte RY; Yagupolskii YL; Yagupolskii LM; Bernhardt E; Willner H; Leito IJ Equilibrium Acidities of Superacids. Org. Chem 2011, 76, 391–395.
16. Pitman CL; Finster ONL; Miller AJM Cyclopentadiene-Mediated Hydride Transfer from Rhodium Complexes. Chem. Commun 2016, 52, 9105–9108.
17. Quintana LMA; Johnson SI; Corona SL; Villatoro W; Goddard WA; Takase MK; VanderVelde DG; Winkler JR; Gray HB; Blakemore JD Proton-Hydride Tautomerism in Hydrogen Evolution Catalysis. Proc. Nat. Acad. Sci. U.S.A 2016, 113, 6409–6414.
18. Peng Y; Ramos-Garcés MV; Lionetti D; Blakemore JD Structural and Electrochemical Consequences of [Cp*] Ligand Protonation. Inorg. Chem 2017, 56, 10824–10831. [PubMed: 28832122]
19. Johnson SI; Gray HB; Blakemore JD; Goddard WA Role of Ligand Protonation in Dihydrogen Evolution from a Pentamethylcyclopentadienyl Rhodium Catalyst. Inorg. Chem 2017, 56, 11375–11386. [PubMed: 28862433]
20. Brintzinger H; Bercaw JE Bis(pentamethylcyclopentadienyl)titanium(II). Isolation and Reactions with Hydrogen, Nitrogen, and Carbon Monoxide. J. Am. Chem. Soc 1971, 93, 2045–2046.
21. O WWN; Lough AJ; Morris RH Bifunctional Mechanism with Unconventional Intermediates for the Hydrogenation of Ketones Catalyzed by an Iridium(III) Complex Containing an N-heterocyclic Carbene with a Primary Amine Donor. Organometallics 2012, 31, 2152–2165.
22. Kefalidis CE; Perrin L; Burns CJ; Berg DJ; Maron L; Andersen RA Can a Pentamethylcyclopentadienyl Ligand Act as a Proton-Relay in F-Element Chemistry? Insights from a Joint Experimental/Theoretical Study. Dalton Trans. 2015, 44, 2575–2587. [PubMed: 25340677]
23 (a). Chalkley MJ; Del Castillo TJ; Matson BD; Roddy JP; Peters JC Catalytic N_2-to-NH_3 Conversion by Fe at Lower Driving Force: A Proposed Role for Metallocene-Mediated PCET. ACS Cent. Sci 2017, 3, 217–223. [PubMed: 28386599] (b)Chalkley MJ; Del Castillo TJ; Matson BD; Peters JC Fe-Mediated Nitrogen Fixation with a Metallocene Mediator: Exploring pKa Effects and Demonstrating Electrocatalysis. J. Am. Chem. Soc 2018, 140, 6122–6129. [PubMed: 29669205]
24. Klingert B; Werner H Basic Metals. XLII. Metal Basicity of the Complexes $C_5Me_5Rh(PMe_3)_2$, $C_5Me_5Rh(C_2H_4)PMe_3$, and $C_5Me_5Rh(C_2H_4)P_2Me_4$: New Pentamethylcyclopentadienyl rhodium(I) and -rhodium(III) Compounds. Chem. Ber 1983, 116, 1450–1462.
25. Faller JW; D'Alliessi DG Tunable Stereoselective Hydrosilylation of PhC≡CH Catalyzed by Cp*Rh Complexes. Organometallics 2002, 21, 1743–1746.
26. Chow P; Zargarian D; Taylor NJ; Marder TB Synthesis of Hydrido-bis(acetylide) Complexes of Rhodium and the Molecular Structures of Mer-trans-$[Rh(PMe_3)_3(H)(C{\equiv}CPh)_2]$ and Mer-trans-$[\{Rh(dmpe)(H)(C{\equiv}CSiMe_3)_2\}_2(\mu\text{-dmpe})]$ (dmpe = $Me_2PCH_2CH_2PMe_2$). J. Chem. Soc., Chem. Commun 1989, 1545–1547.
27. Zhang F; Jia J; Dong S; Wang W; Tung C-H, Organometallics 2016, 35, 1151–1159.
28. Faraone F; Bruno G; Schiavo SL; Tresoldi G; Bombieri G η^5-Cyclopentadienylrhodium(I) complexes containing diphosphines and their reactions with the electrophiles H^+ and Me^+. Crystal and molecular structure of $[Rh(\eta^5\text{-}C_5H_5)(CO)(Ph_2PCH_2PPh_2)]$, a complex with a unidentate bis(diphenylphosphino)methane ligand. J. Chem. Soc., Dalton Trans 1983, 433–438.
29. Klingert B; Werner H Synthesis and Reactivity of $[C_5Me_5Rh(\mu\text{-}PMe_2)]_2$: Addition and Insertion Reactions of Oxygen and its Homologs to the Rh_2P_2 Unit. J. Organomet. Chem 1983, 252, C47–C52.
30. Klingert B; Werner H Metal Complexes with Bridging Dimethylphosphido Ligands. VIII. Protonation of Doubly Bridged Pentamethylcyclopentadienylrhodium(II) Complexes and Subsequent Reactions of the μ-hydridodirhodium Cation $[(C_5Me_5Rh)_2(\mu\text{-}PMe_2)_2(\mu\text{-}H)]^+$. J. Organomet. Chem. 1987, 333, 119–128.

31. Jones WD; Kuykendall VL; Selmeczy AD Ring Migration Reactions of (C_5Me_5) Rh(PMe_3)H_2. Evidence for η3 Slippage and Metal-to-Ring Hydride Migration. Organometallics 1991, 10, 1577–1586.
32. Edelbach BL; Jones WD Mechanism of Carbon-Fluorine Bond Activation by (C_5Me_5) Rh(PMe_3)H_2. J. Am. Chem. Soc 1997, 119, 7734–7742.
33. Gelabert R; Moreno M; Lluch JM; Lledós A; Pons V; Heinekey DM Synthesis and Properties of Compressed Dihydride Complexes of Iridium: Theoretical and Spectroscopic Investigations. J. Am. Chem. Soc 2004, 126, 8813–8822. [PubMed: 15250735]
34 (a). Roy S; Sharma B; Pécaut J; Simon P; Fontecave M; Tran PD; Derat E; Artero V Molecular Cobalt Complexes with Pendant Amines for Selective Electrocatalytic Reduction of Carbon Dioxide to Formic Acid. J. Am. Chem. Soc 2017, 139, 3685–3696. [PubMed: 28206761] (b)Elgrishi N; Kurtz DA; Dempsey JL Reaction Parameters Influencing Cobalt Hydride Formation Kinetics: Implications for Benchmarking H_2-Evolution Catalysts. J. Am. Chem. Soc 2017, 139, 239–244 [PubMed: 27997157]
35. Castillo CE; Stoll T; Sandroni M; Gueret R; Fortage J; Kayanuma M; Daniel C; Odobel F; Deronzier A; Collomb M-N, Inorg. Chem 2018, 57, 11225–11239. [PubMed: 30129361]
36. White C; Yates A; Maitlis PM (η^5-Pentamethylcyclopentadienyl)rhodium and -iridium Compounds. Inorg. Synth 1992, 29, 228–234.
37. Nutton A; Bailey PM; Maitlis PM Pentamethylcyclopentadienylrhodium and -iridium Complexes. Part 29. Syntheses and X-ray Structure Determinations of Tri-μ-hydroxybis[(η-pentamethylcyclopentadienyl)rhodium] Hydroxide Undecahydrate and -iridium Acetate Tetradecahydrate and Related Complexes. J. Chem. Soc., Dalton Trans.: Inorg. Chem 1981, 1997–2002.
38. Dadci L; Elias H; Frey U; Hoernig A; Koelle U; Merbach AE; Paulus H; Schneider JS π-Arene Aqua Complexes of Cobalt, Rhodium, Iridium, and Ruthenium: Preparation, Structure, and Kinetics of Water Exchange and Water Substitution. Inorg. Chem 1995, 34, 306–315.
39. Reinhardt R; Kaim W Complexes of α-diimines with Pentamethylcyclopentadienylrhodium in Different Oxidation States. Z. Anorg. Allg. Chem 1993, 619, 1998–2005.
40. Kaim W; Reinhardt R; Waldhoer E; Fiedler J Electron Transfer and Chloride Ligand Dissociation in Complexes $[(C_5Me_5)ClM(bpy)]^+$/$[(C_5Me_5)M(bpy)]^n$ (M = Co, Rh, Ir; n = 2+, +, 0, −): A Combined Electrochemical and Spectroscopic Investigation. J. Organomet. Chem 1996, 524, 195–202.
41. Lionetti D; Day VW; Blakemore JD Synthesis and Electrochemical Properties of Half-Sandwich Rhodium and Iridium Methyl Complexes. Organometallics 2017, 36, 1897–1905.
42. Blakemore JD; Hernandez ES; Sattler W; Hunter BM; Henling LM; Brunschwig BS; Gray HB Pentamethylcyclopentadienyl Rhodium Complexes. Polyhedron 2014, 84, 14–18.
43. Connelly NG; Geiger WE Chemical Redox Agents for Organometallic Chemistry. Chem. Rev 1996, 96, 877–910. [PubMed: 11848774]
44. Appel AM; Helm ML Determining the Overpotential for a Molecular Electrocatalyst. ACS Catalysis 2013, 4, 630–633.
45 (a). The data provide an estimated Rh–H17 bond distance of 1.76(7) Å. However, the large amount of electron density associated with the rhodium center could lead to underestimation of this bond distance. For more information, see the following reference.Schmidtmann M; Coster P; Henry PF; Ting VP; Weller MT; Wilson CC Determining hydrogen positions in crystal engineered organic molecular complexes by joint neutron powder and single crystal X-ray diffraction. CrystEngComm 2014, 16, 1232–1236.
46. Wayland BB; Ba S; Sherry AE Activation of Methane and Toluene by Rhodium(II) Porphyrin Complexes. J. Am. Chem. Soc 1991, 113, 5305–5311.
47. Simoes JAM; Beauchamp JL Transition Metal-Hydrogen and Metal-Carbon Bond Strengths: the Keys to Catalysis. Chem. Rev 1990, 90, 629–688.
48. Warren JJ; Tronic TA; Mayer JM Thermochemistry of Proton-Coupled Electron Transfer Reagents and its Implications. Chem. Rev 2010, 110, 6961–7001. [PubMed: 20925411]
49. Waldie KM; Ostericher AL; Reineke MH; Sasayama AF; Kubiak CP Hydricity of Transition-Metal Hydrides: Thermodynamic Considerations for CO_2 Reduction. ACS Catal. 2018, 8, 1313–1324.

50. Dempsey JL; Winkler JR; Gray HB Mechanism of H_2 Evolution from a Photogenerated Hydridocobaloxime. J. Am. Chem. Soc 2010, 132, 16774–16776. [PubMed: 21067158]
51. Chambers MB; Kurtz DA; Pitman CL; Brennaman MK; Miller AJM Efficient Photochemical Dihydrogen Generation Initiated by a Bimetallic Self-Quenching Mechanism. J. Am. Chem. Soc 2016, 138, 13509–13512. [PubMed: 27673375]
52. Creutz C Bipyridine Radical Ions. Comments Inorg. Chem 1982, 1, 293–311.
53. Bock H; Lechner-Knoblauch U; Hänel P Radical Ions. 70. The Effect of Phosphorus Substituents on the Cyclic Voltammetric Reduction of Aromatic π-systems. Chem. Ber 1986, 119, 3749–3765.
54. Price AJ; Ciancanelli R; Noll BC; Curtis CJ; DuBois DL; DuBois MR HRh(dppb)$_2$, a Powerful Hydride Donor. Organometallics 2002, 21, 4833–4839.
55. Liao JL; Devereux Leon R; Fox MA; Yang CC; Chiang YC; Chang CH; Lee GH; Chi Y Role of the Diphosphine Chelate in Emissive, Charge-Neutral Iridium(III) Complexes. Chem. – Eur. J 2017, 24, 624–635. [PubMed: 29027287]
56. Zhang X-X; Wayland BB Rhodium(II) Porphyrin Bimetalloradical Complexes: Preparation and Enhanced Reactivity with CH_4 and H_2. J. Am. Chem. Soc 1994, 116, 7897–7898.
57. Fulmer GR; Miller AJM; Sherden NH; Gottlieb HE; Nudelman A; Stoltz BM; Bercaw JE; Goldberg KI NMR Chemical Shifts of Trace Impurities: Common Laboratory Solvents, Organics, and Gases in Deuterated Solvents Relevant to the Organometallic Chemist. Organometallics 2010, 29, 2176–2179..
58. Harris RK; Becker ED; Cabral De Menezes SM; Goodfellow R; Granger P NMR Nomenclature. Nuclear Spin Properties and Conventions for Chemical Shifts (IUPAC Recommendations 2001). Pure Appl. Chem 2001, 73, 1795–1818.
59. Harris RK; Becker ED; Cabral De Menezes SM; Granger P; Hoffman RE; Zilm KW Further Conventions for NMR Shielding and Chemical Shifts (IUPAC Recommendations 2008). Pure Appl. Chem 2008, 80, 59–84.

Synopsis

Electrochemical reduction of a [Cp*Rh] hydride leads to H_2 evolution, whereas direct protonolysis does not, providing new insight into the redox-promoted reactivity of half-sandwich rhodium complexes.

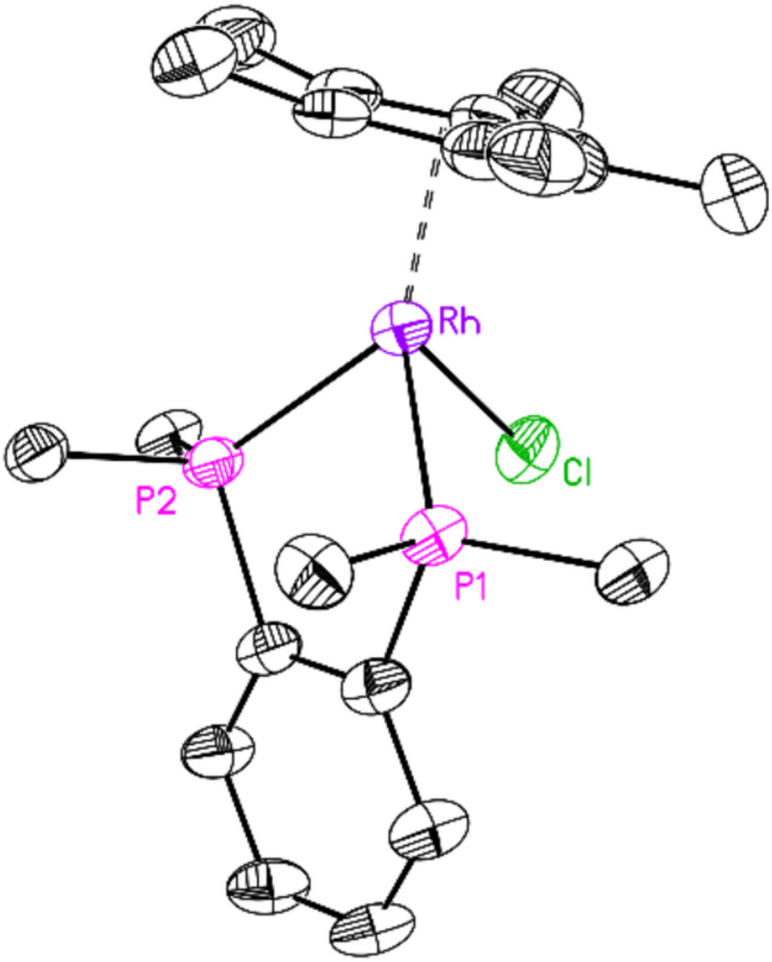

Figure 1.
Crystal structure of **1**. H atoms, PF_6 counteranion, and terminal phenyl groups omitted for clarity.

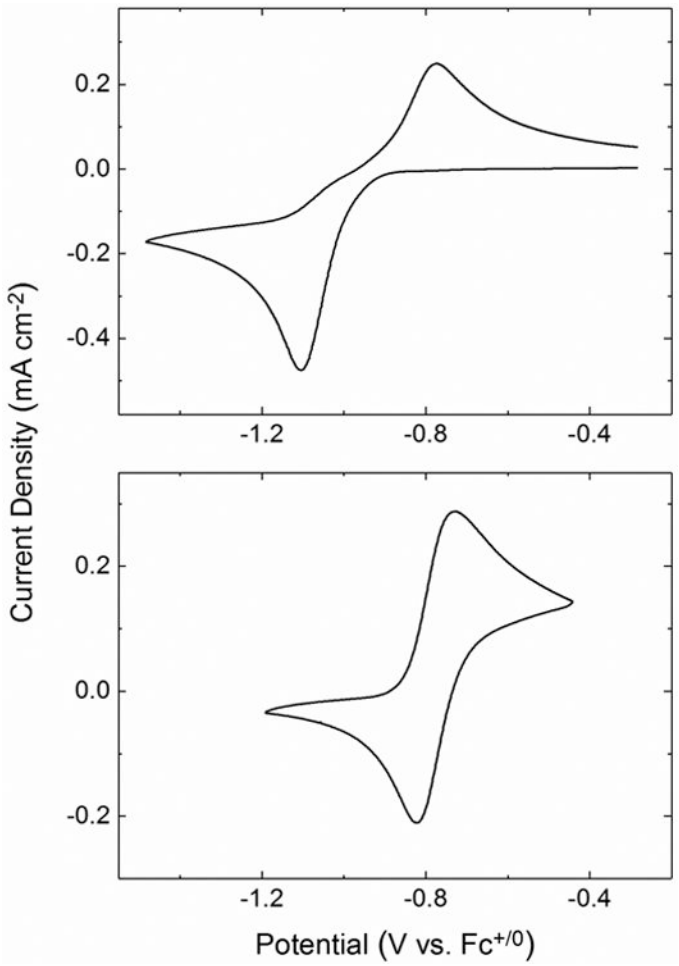

Figure 2.

Cyclic voltammetry of **1** (upper panel, 1 mM) and **2** (lower panel, 1 mM). Electrolyte: 0.1 M $TBAPF_6$ in MeCN, scan rate: 100 mV/s, electrode: highly oriented pyrolytic graphite. The initial potential of the voltammogram of **1** (upper panel) is at ca. −0.30 V, and the initial potential of the voltammogram of **2** (lower panel) is at ca. −1.2 V.

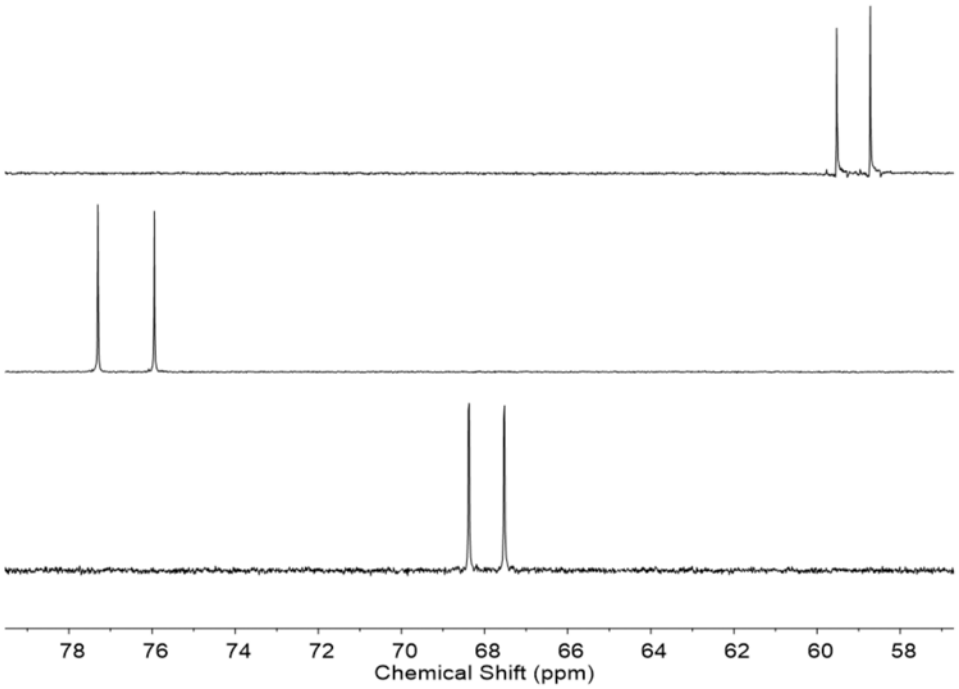

Figure 3.

$^{31}P\{^{1}H\}$ NMR (162 MHz) of **1** (top, CD_3CN, $^{1}J_{P,Rh}$ = 131 Hz), **2** (middle, C_6D_6, $^{1}J_{P,Rh}$ = 220 Hz), and **3** (bottom, CD_3CN, $^{1}J_{P,Rh}$ = 138 Hz).

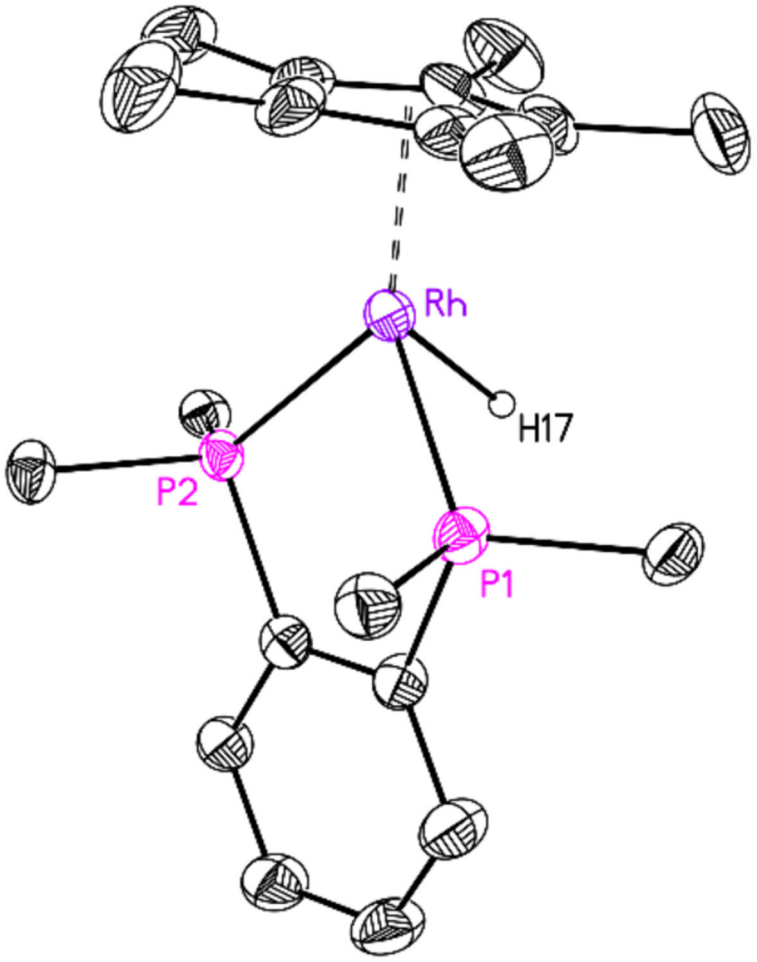

Figure 4.

Crystal structure of **3**. All H atoms not bound to Rh, outer-sphere triflate counteranion, and terminal phenyl groups omitted for clarity.

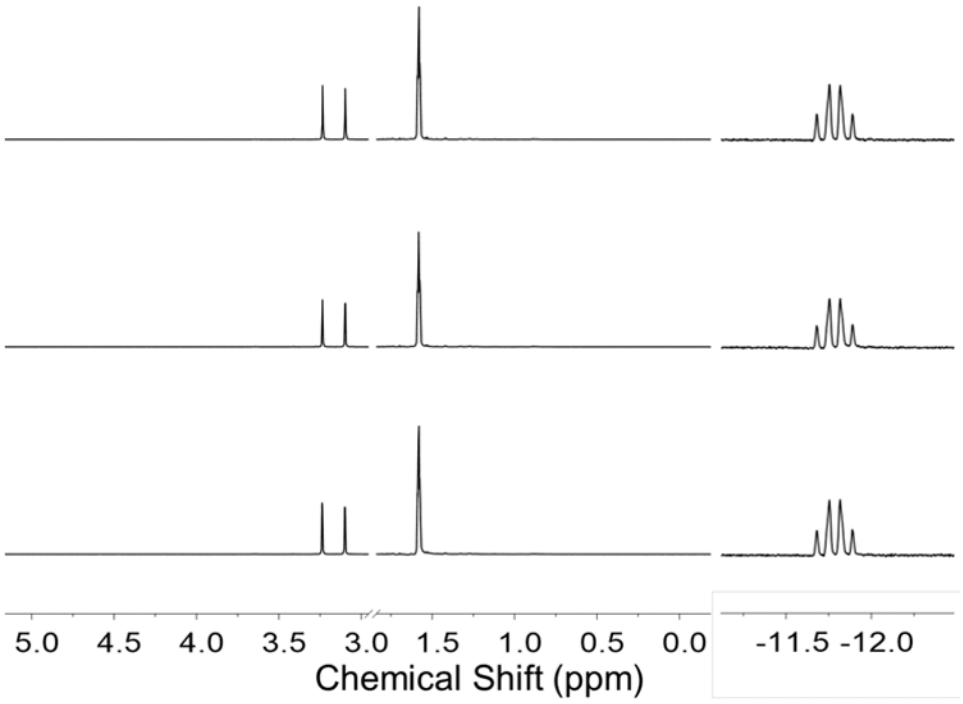

Figure 5.

Partial ^{1}H NMR spectra of a 1:1 mixture of **3** and [DMFH][OTf] in CD_3CN after 15 min (lower panel), 24 hrs (middle), and 48 hrs (upper).

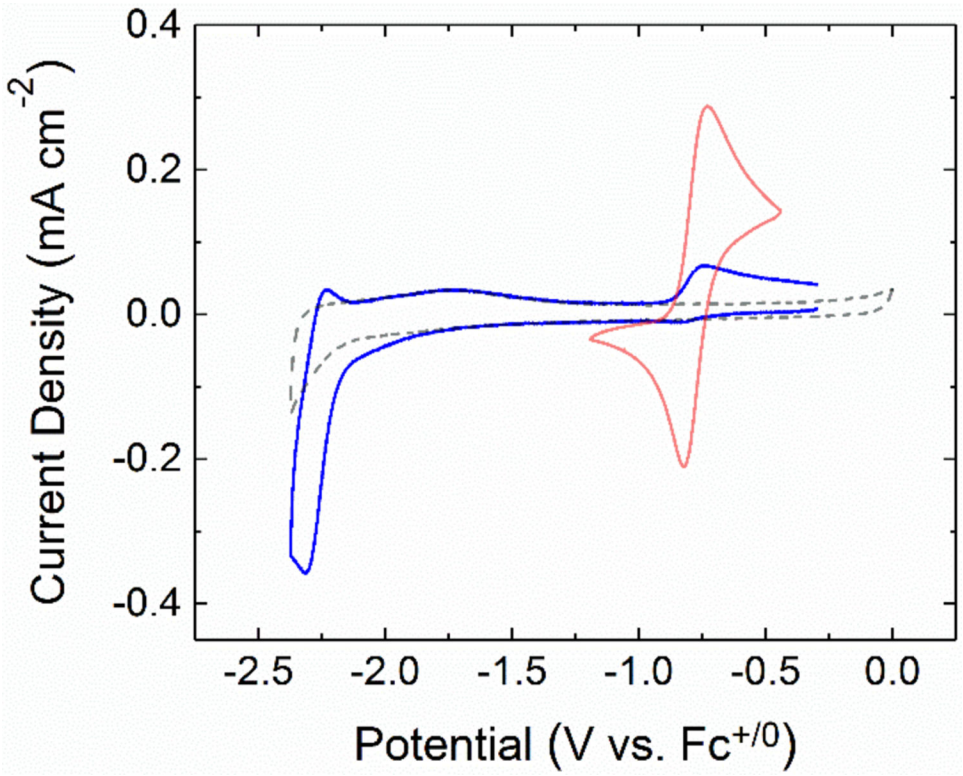

Figure 6.

Red: Cyclic voltammetry of **2** (red, 1 mM), **3** (blue, 1 mM), and a blank (dashed). Electrolyte: 0.1 M $TBAPF_6$ in MeCN, scan rate: 100 mV/s, electrode: highly oriented pyrolytic graphite. The initial potentials of the voltammograms are as follows: for **2**, −1.2 V; for **3**, −0.30 V; for the blank, 0 V.

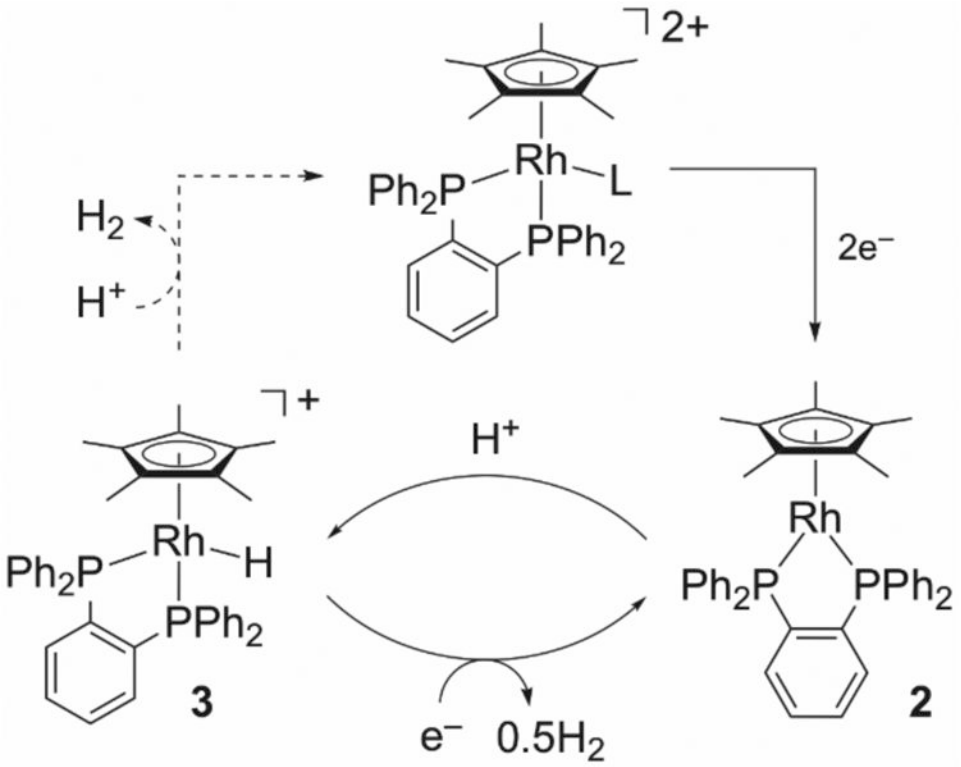

Figure 7.

H_2 evolution chemistry with the Cp*Rh(dppb) platform. Dashed arrows indicate an inactive pathway for H_2 production involving protonolysis of hydride **3**.

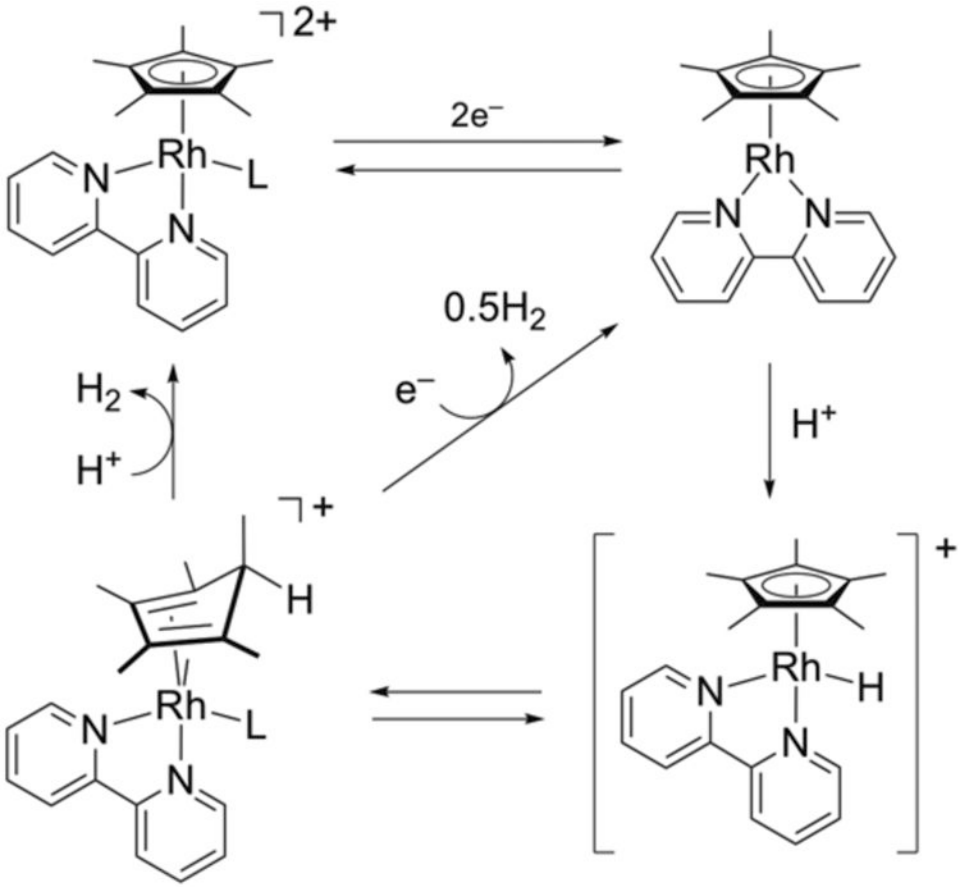

Scheme 1.

H_2 evolution catalyzed by Cp*Rh(bpy). L = halide or coordinated solvent (e.g., MeCN).

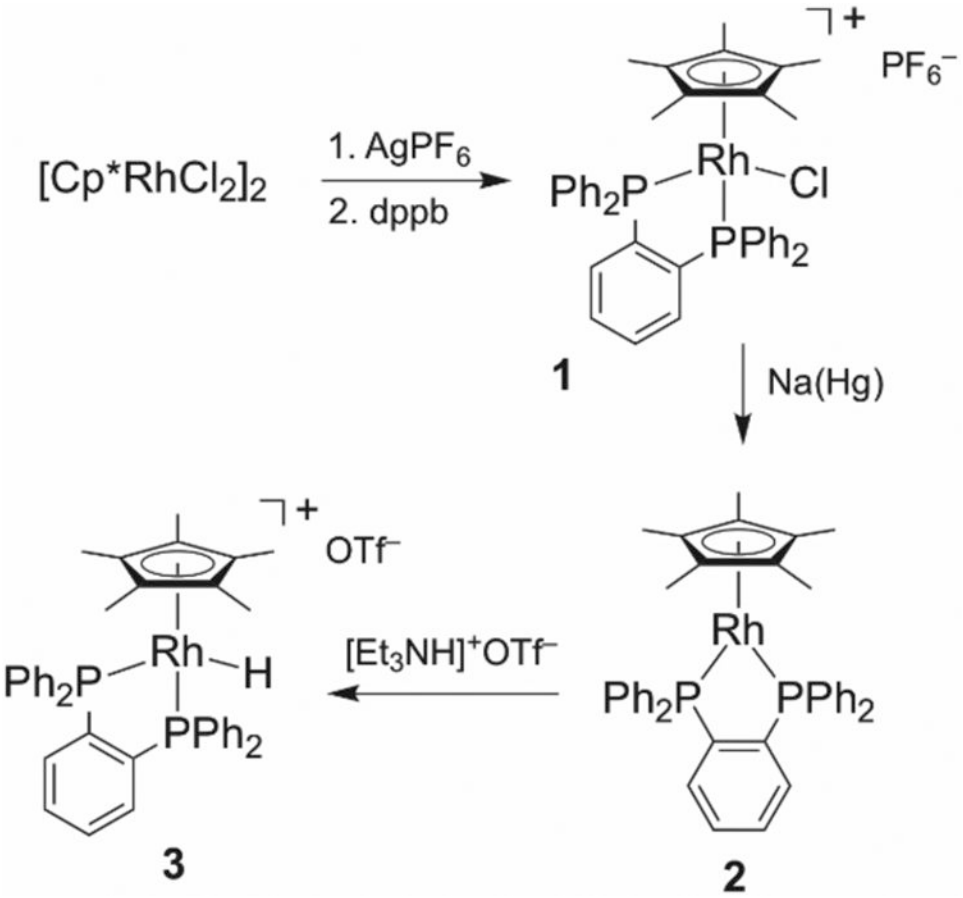

Scheme 2.
Preparation of Cp*Rh complexes.